On the impact of connected automated vehicles in freeway work zones: A cooperative cellular automata model based approach

On the impact of connected automated vehicles in freeway work zones: a cooperative cellular automata model based approach

Yun Zou
School of Civil and Environmental Engineering, Faculty of Engineering and Information Technology, University of Technology Sydney, Sydney, Australia, and
Xiaobo Qu
Department of Architecture and Civil Engineering, Chalmers University of Technology, Gothenburg, Sweden

Abstract

Purpose – Freeway work zones have been traffic bottlenecks that lead to a series of problems, including long travel time, high-speed variation, driver's dissatisfaction and traffic congestion. This research aims to develop a collaborative component of connected and automated vehicles (CAVs) to alleviate negative effects caused by work zones.

Design/methodology/approach – The proposed cooperative component is incorporated in a cellular automata model to examine how and to what scale CAVs can help in improving traffic operations.

Findings – Simulation results show that, with the proposed component and penetration of CAVs, the average performances (travel time, safety and emission) can all be improved and the stochasticity of performances will be minimized too.

Originality/value – To the best of the authors' knowledge, this is the first research that develops a cooperative mechanism of CAVs to improve work zone performance.

Keywords Connected and automated vehicles, Cooperative cellular automata model, Microscopic traffic flow models, Work zone

Paper type Research paper

Nomenclature

$G_{n,t}$	= The front gap of vehicle n at time t;
x_{wz}	= The longitudinal location of work zone;
$x_{n,t}$	= The longitudinal location of left front point on vehicle n at time t;
$y_{n,t}$	= The lateral location of left front point on vehicle n at time t;
L_t	= The length of transition area;
l_n	= The length of vehicle n;
$t_{n,t}$	= The headway of vehicle n at time t;
t_{acc}	= The interaction headway;
$a(V_{n,t})$	= The acceleration rate of vehicle n at time t;
$B_{n,t}$	= The brake status of vehicle n at time t;
$V_{n,t}$	= The velocity of vehicle n at time t;
$V_{limit,n,t}$	= The speed limitation of vehicle n at time t;
$G_{eff,n,t}$	= The effective front gap of vehicle n at time t;
$G_{wz,n,t}$	= The distance from the front bumper of vehicle n to work zone at time t;
$G_{security}$	= The safety distance;
$p(f_L, f_H, L_a, L_t)$	= The randomization probability within work zone;
f_L	= The traffic flow volume of light vehicles;
f_H	= The traffic flow volume of heavy vehicles;
L_a	= The length of activity area;
$G_{n,f,t}$	= The front gap of vehicle n with front neighboring vehicle at time t;
P_{merge}	= The possibility of merging maneuver;
$\delta_{n,t}$	= Maximum allowable deceleration of vehicle n at time t;
TTC	= The time left to collision; and
$D_{comfort}$	= The comfortable deceleration rate.

1. Introduction

A work zone is a partially closed road section due to periodic maintenance, rehabilitation and reconstruction, bringing negative impacts on traffic performance, such as, accident, congestion, long travel time and dissatisfaction among road

The current issue and full text archive of this journal is available on Emerald Insight at: **www.emeraldinsight.com/2399-9802.htm**

Journal of Intelligent and Connected Vehicles
1/1 (2018) 1–14
Emerald Publishing Limited [ISSN 2399-9802]
[DOI 10.1108/JICV-11-2017-0001]

The authors would like to thank University of Technology Sydney (UTS) for providing the scholarship.

Received 20 November 2017
Revised 18 February 2018
Accepted 3 April 2018

users (Meng and Weng, 2011). The number of the through lanes declines; as a result, the traffic capacity is significantly reduced because of not only lane closure but also lane-changing activities (Laval and Daganzo, 2006; Qu *et al.*, 2015). Vehicles on non-through lanes have to merge into through lanes; otherwise, vehicles need to decelerate or even stop due to the existence of the work zone; in other words, lane-changing maneuvers become compulsory for those vehicles on non-through lanes. It makes the situation even worse when a large number of vehicles merge into a same target lane without cooperation. Indeed, the presence of a work zone can increase not only the possibility of traffic accidents happening but also the travel time due to the boost of density (Wang *et al.*, 1996; Rouphail *et al.*, 1988; Khattak *et al.*, 2002; Garber and Zhao, 2002; Meng and Weng, 2011).

With the continuous increase of the travel demand, traffic flow becomes more unstable and vulnerable. During peak hours, even a slight disturbance imposes high possibility of causing severe traffic interruptions, as human drivers are more likely to make heterogeneous responses under these conditions (Qu *et al.*, 2017). It has been well recognized that these human driver's limit and heterogeneity are essentially non-controllable in traffic operations. Macadam (2003) proposed that human drivers show obvious reaction delay in reacting to different indications, such as merge indications and brake indications; moreover, the intensity of an indication has to reach a threshold to be sensed by human drivers. In this regard, transportation researchers develop models and applications that are very robust to accommodate these limit and heterogeneity, which lead to low capacity of our transport systems. With the advent of the connected and automated vehicles (CAV), the cooperation among vehicles becomes possible and, as a result, the limit and the heterogeneity can be controlled through developing a cooperative vehicle motion controlling system that is able to smooth our traffic flow dynamics (Zhou *et al.*, 2017a, 2017b).

There are a few studies analyzing the influences caused by work zones. Adeli and Jiang (2003) used a neuro-fuzzy logic model to estimate the work zone capacity on the freeway. Jiang and Adeli (2004a, b) used clustering-neural network models to estimate the work zone capacity on the freeway with less than 10 per cent error and applied object-oriented model to estimate the freeway work zone capacity, as well as queue delay. Meng and Weng (2011) proposed an improved cellular automata (ICA) model to simulate the work zone traffic flow dynamics. Weng and Meng (2014) proposed a methodology to estimate the rear-end crash possibility on the work zone merging area, and it is found that this possibility increases as a result of late merging which is an instant merging maneuver with short front gap to the activity area in a work zone. Weng and Yan (2016) established a truncated lognormal distribution method to estimate the traffic capacity due to the presence of work zone. To the best of our knowledge, there is no research that applies CAVs' smoothing work zone traffic flow dynamics. CAVs are able to make immediate reaction to the deceleration of the leading vehicle; therefore, shorter headways are required. Moreover, an embedded computer is able to compute the optimal safe speed as well as sliding distance to narrow the front gap, which is almost impossible for human drivers to calculate. As such, the average travel time to go through the work zone and the speed oscillation are anticipated to be reduced as the penetration rate of CAVs goes up if a proper collaborative mechanism is well designed. In this research, to bridge this void, we propose a cooperative cellular automata model (CCAM) based on the ICA model developed by Meng and Weng (2011).

The paper is organized as follows. In Section 2, the configuration of work zone from cellular automata model and a study area on Pacific Highway are demonstrated, followed by a review of ICA model with an amendment at the end. Section 3 describes the proposed microscopic traffic flow model for CAVs with the cooperative component among vehicle illustrated in detail. Section 4 presents the performance indicators, including traffic delay, safety and vehicle emission, under various penetration rates of CAVs. The last section concludes the paper.

2. Model development to simulate the movement of the manually driven vehicle

2.1 Site description

This research is established on the basis of a two-lane (in one direction) freeway with a work zone at the Lane 1 starting from longitudinal location x_1 to x_4 as shown in Figure 1(a). The speed limit on this freeway is 110 km/h before vehicle entering advance warning zone that is from longitudinal location x_0 to x_1. The speed limit turns to 80 km/h after reaching the advance warning sign which is located at x_0, and it then reduces to 60 km/h when vehicles enter the work zone. Figure 1(b) shows a photo of a work zone located on Pacific Highway around Coolangatta airport, where the number of lanes drops from two to one because of a large scale of construction tasks as indicated by the circle.

2.2 Modified ICA model

To simulate the traffic flow dynamics of MVs, the ICA model is used with modifications to incentive and safety criteria. According to the ICA model, lanes are divided into cells of 0.5 m in length and 0.7 m in width. $G_{n,t}$ denotes the front gap between vehicle n and its leading vehicle $n-1$ or a work zone at time t; thus, for any two sequential vehicles:

$$G_{n,t} = x_{n-1,t} - x_{n,t} - l_{n-1} \tag{1}$$

Similarly, $G_{wz,n,t}$ denotes the front gap between vehicle n and the work zone ahead; thus:

$$G_{wz,n,t} = x_{wz} - x_{n,t} + y_{n,t} \times L_t/5 \tag{2}$$

2.2.1 Acceleration

If time headway $t_{n,t}$ is greater than interaction headway t_{acc} or neither vehicle n nor its leading vehicle $n-1$ has braked (B = 0 otherwise B = 1) during the previous simulation interval $t-1$, vehicle n accelerates with acceleration rate of $a(V_{n,t})$. Namely, if $(B_{n,t-1} = 0 \bigwedge B_{n-1,t-1} = 0) \bigvee t_{n,t} > t_{acc}$:

$$V_{n,t} = \min\{V_{n,t-1} + a(V_{n,t}), V_{limit,n,t}\} \tag{3}$$

Here, $a(V_{n,t})$ is a function of current speed $V_{n,t}$, and the values under different speeds are demonstrated in Table II. $V_{limit,n,t}$ denotes the current speed limitation.

Figure 1 A plan view of freeway section around a work zone and a work zone on pacific highway

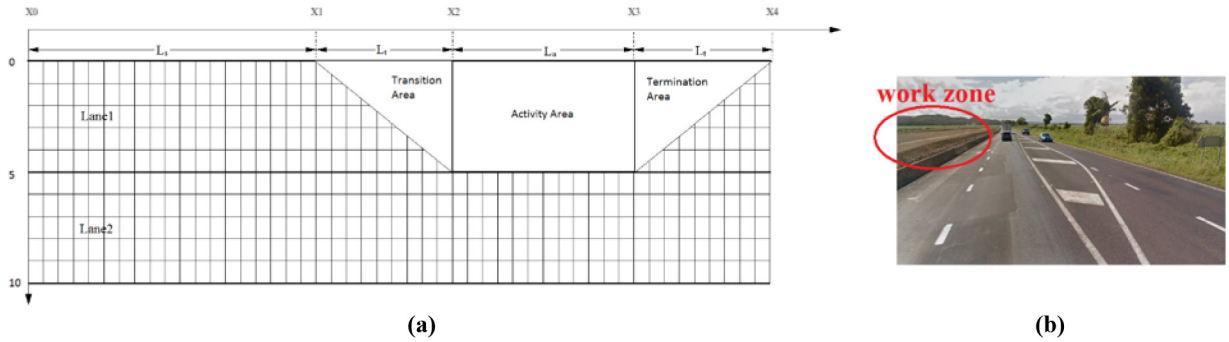

(a) **(b)**

2.2.2 Deceleration

Compared with the original CA model, the ICA model proposed a new concept that is effective front gap, taking the movement of vehicle $n-1$ into account:

$$G_{eff,n,t} = G_{n,t} + \max\{0, \min(V_{n-1,t-1}, \quad G_{n-1,t}) - G_{security}\} \tag{4}$$

where the component $\min(V_{n-1,t-1}, G_{n-1,t})$ denotes the anticipated velocity of the leading vehicle.

If $Geff_{n,t} < V_{n,t}$, vehicle n decelerates to avoid rear-end crash with its leading vehicle or the merging vehicle. The target velocity for the deceleration period is $Geff_{n,t}$ instead of $G_{n,t}$, which is too conservative, namely:

$$V_{n,t} = \min(V_{n,t}, G_{eff,n,t}) \tag{5}$$

If $V_{n,t} < V_{n,t-1}$, vehicle n decelerated with brake status activated, namely, $B_{n,t} = 1$.

2.2.3 Randomization probability

Randomization probability was first proposed in Nagel–Schrechenberg's CA model to simulate the excessive brake and acceleration delay, which simulates the human limit as traffic flow forward (Nagel and Schreckenberg, 1992). Meng and Weng (2010) pointed out that the randomization probability is a function of traffic flow of light vehicles, traffic flow of heavy vehicles, the length of activity area and the length of transition area:

$$P(f_L, f_H, L_a, L_t) = \mathrm{a}f_L + \mathrm{b}f_H + \mathrm{c}L_a + \mathrm{d}L_t + \mathrm{e} \tag{6}$$

Parameters in equation (6) were calibrated by Meng and Weng (2010) using a trial-and-error method as demonstrated in Table I.

2.2.4 Incentive criterion

In the ICA model, two incentive criteria are proposed, which are $V_{n,t} > G_{n,t} \wedge V_{n,t} > V_{n-1,t}$ and $G_{n,t} < G_{n,f,t}$. However, the dominating incentive ahead of a work zone is the distance to the transition area. In that case, vehicles are encouraged to merge into the through lane as $G_{wz,n,t}$ reaches a critical value. Hidas (2002) proposed that lane-changing action becomes essential when the headway to a lane blockage is less than 8 s. Based on this, we propose equation (7) to calculate the possibility of lane-changing action in this research:

Table I Comparison between ICA and modified ICA

Variable	ICA model	Modifications in CCAM
Randomization probability	Both are determined by function that is illustrated in equation (6), and the parameters are demonstrated in Table II.	
Allowed maximum speed	45 cell/s within a work zone 60 cell/s elsewhere	Illustrated in Table III
Acceleration	Both are determined by brake status and headway	
Deceleration	Determined by effective front gap	The effective front gap is modified as shown in equation 14
Incentive criterion	Encouraged by a larger front gap	Encouraged by the distance to the work zone
Safety criterion	Exclude the influence of the front gap with the ALV	Include the influence of the front gap with the ALV

$$P_{merge} = \begin{cases} 0, & if \ G_{wz,n,t} > 8 \times V_{limit,n,t} \\ 1, & if \ G_{wz,n,t} \le 8 \times V_{limit,n,t} \end{cases} \tag{7}$$

2.2.5 Safety criterion

As mentioned in the ICA model, the value of the gap between vehicle n and its back neighboring vehicle in the target lane needs to be greater than the value of the maximum speed, namely, $G_{n,b,t} > V_{limit,n,t}$ (Meng and Weng, 2011). However, this safety criterion excludes the gap between subject vehicle and its anticipated leading vehicle (ALV), which is unrealistic. To avoid rear-end crash during merging period, a merging vehicle has to maintain enough gap with its ALV; therefore, this gap needs to start from a reasonable value to accommodate the speed difference.

We propose a new safety criterion in CCAM, that is, the front gap with the ALV from through lane has to be greater than $R_c(V_{n,t} - V_{alv,t}) + G_{security}$ to accommodate the speed difference. Here, R_c denotes the reaction time, and it is assumed to be 1 s. With regard to lateral speed, it is limited to be less than two cells per second according ICA (Meng and Weng, 2011). However, merging maneuver is assumed to be completed within 1 s in CCAM, which means vehicles are able to merge into the target lane during the next simulation interval as long as conditions are fulfilled. To better compare the performances of ICA and

CCAM, MVs are assumed to be able to finish merging maneuver with 1 s as well, and the main differences between the ICA model and the CCAM are compared in Table I.

3. Model development to simulate movements of connected and automated vehicles

3.1 Following model

3.1.1 Maximum allowable deceleration

In this model, we propose a concept named the maximum allowable deceleration. The maximum allowable deceleration $\delta_{n,t}$ is defined as the maximum disturbance that a traffic state could accommodate, and $d_{n,t}$ denotes the disturbance that vehicle n suffers at time t. If $V_{n+1,t} > V_{n,t} - d_{n,t}$, there is a risk that rear-end crash occurs between vehicle n and its following vehicle; otherwise, a rear-end crash is able to be avoided. In that case, the maximum allowable deceleration needs to be considered only if $V_{n+1,t} > V_{n,t} - d_{n,t}$.

If both vehicles maintain the same speed for the following simulation intervals, the time to collision (TTC) under such disturbance $\delta_{n,t}$ is calculated as:

$$TTC = \frac{G_{n+1,t}}{V_{n+1,t} - (V_{n,t} - d_{n,t})} \tag{8}$$

Let τ be the threshold of time to collision. Only if $\frac{G_{n+1,t}}{V_{n+1,t} - (V_{n,t} - d_{n,t})} \geq \tau$, can a crash be avoided. To rearrange the equation:

$$d_{n,t} \leq (V_{n,t} - V_{n+1,t}) + \frac{G_{n+1,t}}{\tau} \tag{9}$$

Thus:

$$\delta_{n,t} = (V_{n,t} - V_{n+1,t}) + \frac{G_{n+1,t}}{\tau} \tag{10}$$

Then $\delta_{n,t}$, the maximum disturbance that a car following scenario can accommodate, can be calculated. This disturbance can be used to determine the optimal speeds as depicted in the following section.

3.1.2 Optimal speed increment

As CAV n narrows the front gap with its leading vehicle $n-1$, a speed difference between these two successive vehicles are computed as optimal speed increments; With these computations, the following vehicles are able to not only reduce the headway at highest efficiency but also avoid rear-end crash even when the leading vehicle brakes immediately. The worst condition results from the leading CAV's maximum deceleration rate that is the lesser of aforementioned disturbance $\delta_{n-1,t}$ and the comfortable deceleration rate; thus, the minimum possible stopping distance for vehicle n at the current simulation interval is $G_{n,t} + V_{n-1,t} - \min(\delta_{n-1,t}, D_{comfort})$. Here, $V_{n-1,t} - \min(\delta_{n-1,t}, D_{comfort})$ denotes the minimum possible velocity of the leading vehicle and the target velocity of vehicle n. The maximum velocity for vehicle n narrowing the gap is $V_{n-1,t} + \Delta_{n,t}$, where $\Delta_{n,t}$ denotes the optimal speed increment; thus, the equation can be written as:

$$\begin{aligned}&(\Delta_{n,t} + V_{n-1,t})^2 - (V_{n-1,t} - \min(\delta_{n-1,t}, D_{comfort}))^2 \\ &= 2(G_{n,t} + V_{n-1,t} - \min(\delta_{n-1,t}, D_{comfort}))D_{comfort}\end{aligned} \tag{11}$$

That is:

$$\Delta_{n,t} = \sqrt{2(G_{n,t} + V_{n-1,t} - min(\delta_{n-1,t}, D_{comfort}))D_{comfort} + (V_{n-1,t} - \min(\delta_{n-1,t}, D_{comfort}))^2} - V_{n-1,t} \tag{12}$$

3.1.3 Effective gap

Case 1: if leading vehicle is an MV

If the leading vehicle $n-1$ is an MV rather than a CAV, the subject CAV n will not expect more information from its leading vehicle. Thus, a same equation from ICA model is used to calculate the effective gap, namely:

$$G_{eff,n,t} = G_{n,t} + \max\{0, \min(V_{n-1,t-1}, \quad G_{n-1,t}) - G_{security}\} \tag{13}$$

Case 2: if leading vehicle is a CAV

If two successive vehicles are both CAVs, the effective gap of the leading vehicle can be sent to its following vehicle; therefore, we modified the effective gap as follow:

$$G_{eff,n,t} = G_{n,t} + \max\{0, \min(V_{n-1,t}, \quad G_{eff,n-1,t}) - G_{security}\} \tag{14}$$

In this equation (14), $V_{n-1,t}$ is used to calculate the anticipated speed of leading vehicle instead of $V_{n-1,t-1}$ which is applied in equation (13), because the leading CAV $n-1$ is able to share the speed with its surrounding CAVs accurately with negligible delay. In addition, an updated effective gap is sent from the leading CAV $n-1$ to the subject CAV n for the effective gap calculation, which enables two sequential CAVs to travel with a shorter gap so as to increase the traffic capacity.

3.1.4 Deceleration

The velocity of a CAV is mainly determined by both the front gap and the relative speed to its leading vehicle. CAVs will brake if its leading vehicle decelerates and the current front gap is relatively small, namely, if $B_{n-1,t} = 1 \wedge G_{n,t} <= \alpha V_{n,t-1}$, $B_{n,t} = 1$. Here α is calibrated to be 2 s. The assumption is that CAVs regard two sequential brakes that can potentially indicate the congestion downstream. In that case, if $G_{n,t} > 2 \times V_{n,t-1}$, there will be two possible scenarios depending the brake status.

Scenario 1: if the leading vehicle's brake status during next simulation interval is not activated, $G_{n,t+1}$ is definitely acceptable for the subject vehicle to keep its following action.

Scenario 2: if the leading vehicle's brake status during next simulation interval is activated, the front gap which is more than the value of $V_{n,t-1}$ (thus the effective gap is definitely

greater than the current velocity) is enough for a CAV decelerate or even stop.

Trajectories extracted from simulations have proved that rear-end crash can be avoided when α is equal to two.

If $G_{eff,n,t} < V_{n,t}$, vehicle n decelerates to $G_{eff,n,t}$ avoid rear-end crash with its leading vehicle $n-1$, namely, $V_{n,t} = \min(V_{n,t}, G_{eff,n,t})$; moreover, a CAV will decelerate if its surrounding vehicles need cooperation as illustrated in the lane-changing model. If $V_{n,t} < V_{n,t-1}$, vehicle n decelerates with brake status activated: $(B_{n,t} = 1)$.

3.1.5 Narrowing the front gap

$G_{security}$ is introduced into CCAM from the ICA model to ensure that CAVs can decelerate to a safe speed before rear-end crash happens with a relatively small deceleration rate for comfort consideration. If vehicle n has a greater velocity than its leading vehicle when the front gap is greater than the safety distance, the velocity of vehicle n is allowed to be greater than that of its leading vehicle by one speed increment; however, the velocity should be less than the effective gap to avoid a rear-end crash. Namely, If $G_{n,t} > G_{security} \wedge V_{n,t-1} > V_{n-1,t}$:

$$V_{n,t} = \min(V_{n-1,t} + \Delta_{n,t},\ G_{eff,n,t}) \tag{15}$$

At the same time, vehicle n can avoid the necessity of excessive brakes.

If the velocity of vehicle n is less or equal to that of vehicle n-1 when the front gap is greater than the safety distance, there are two scenarios:

1 *Scenario 1:* when the brake status of vehicle n is not activated, vehicle n accelerates by acceleration rate proposed in the ICA model; however, the speed difference should not be greater than one speed increment, namely, If $G_{n,t} > G_{security} \wedge B_{n,t} \neq 1 \wedge V_{n,t-1} \leq V_{n-1,t}$:

$$V_{n,t} = \min\left(V_{n,t-1} + a(V_{n,t-1}), V_{n-1,t} + \Delta_{n,t}\right) \tag{16}$$

2 *Scenario 2:* when the brake status is activated, vehicle n keeps a lesser speed of $V_{n,t-1}$ and $V_{n-1,t-1}$, that is, if $G_{n,t} > G_{security} \wedge B_{n,t} = 1 \wedge V_{n,t-1} \leq V_{n-1,t}$:

$$V_{n,t} = \min(V_{n,t-1}, V_{n-1,t-1}) \tag{17}$$

3.2 Lane-changing model

Case 1: The ALV and the anticipated following vehicle (AFV) are both CAVs, where the ALV and AFV are the leading vehicle and the following vehicle after the subject vehicle merging into the through lane.

If $G_{n,alv,t} \geq G_{security} \wedge G_{n,afv,t} \geq G_{security}$, vehicle n is able to start merging.

Otherwise, if $G_{n,alv,t} < G_{security}$:

$$V_{n,t} = V_{n,t-1} - \min(D_n, D_{comfort}, \delta_{n,t}) \tag{18}$$

and if $G_{n,afv,t} < G_{security}$:

$$V_{afv,t} = V_{afv,t-1} - \min(D_{afv}, D_{comfort}, \delta_{afv,t}) \tag{19}$$

Here, $G_{n,alv,t}$ and $G_{n,afv,t}$ indicate the gap with ALV and AFV, respectively. If a CAV receives a message of an oncoming work zone from the leading vehicles of its platoon, a merging maneuver is indicated by this CAV. Both ALV and AFV receive the message of this merging maneuver. When CAV starts merging, ALV updates its maximum allowable deceleration by taking $G_{n,alv,t}$ and $V_{n,t}$ into account. At the meanwhile, AFL also updates its front gap to $G_{n,afv,t}$, and the front gap of the CAV is equal to the lesser of $G_{n,alv,t}$ and $G_{n,t}$; thus, maximum allowable deceleration, optimal speed increments and effective gaps of these three vehicles are updated.

Table II Parameters in randomization probability equation

Coefficient	p_{in}	p_{out}
a	-1.24×10^{-4}	-6.80×10^{-5}
b	-1.30×10^{-4}	-1.28×10^{-4}
c	-3.00×10^{-5}	0
d	0	0
e	0.425	0.541

Source: Meng and Weng (2011)

Table III General coefficients

Variable	Condition	MV	CAV
Acceleration rate (cell/s^2)	$V_{n,t-1} \leq 11 cell/s$	4	4
	$11 cell/s < V_{n,t-1} \leq 22 cell/s$	3	3
	$V_{n,t-1} > 22 cell/s$	2	2
Deceleration rate (cell/s^2)		6	6
Comfortable deceleration rate (cell/s^2)		6.8	6.8
Interaction headway (s)		6	6
Safety distance (cell)		9	9
Maximum speed (cell/s)	freeway	Based on equation (24)	60
	freeway work zone	Based on equation (24)	45

Table IV Coefficients of VT-micro model

Coefficients	Constant	Speed	Speed^2	Speed^3
Positive acceleration				
Constant	−0.87605	0.03627	−0.00045	2.55E-06
Acceleration	0.081221	0.009246	−0.00046	4.00E-06
Acceleration^2	0.037039	−0.00618	2.96E-04	−1.86E-06
Acceleration^3	−0.00255	0.000468	−1.79E-05	3.86E-08
Negative acceleration				
Constant	−0.75584	0.021283	−0.00013	7.39E-07
Acceleration	−0.00921	0.011364	−0.0002	8.45E-07
Acceleration^2	0.036223	0.000226	4.03E-08	−3.5E-08
Acceleration^3	0.003968	-9E-05	2.42E-06	−1.6E-08

Figure 2 Deterministic indicators over penetration rate

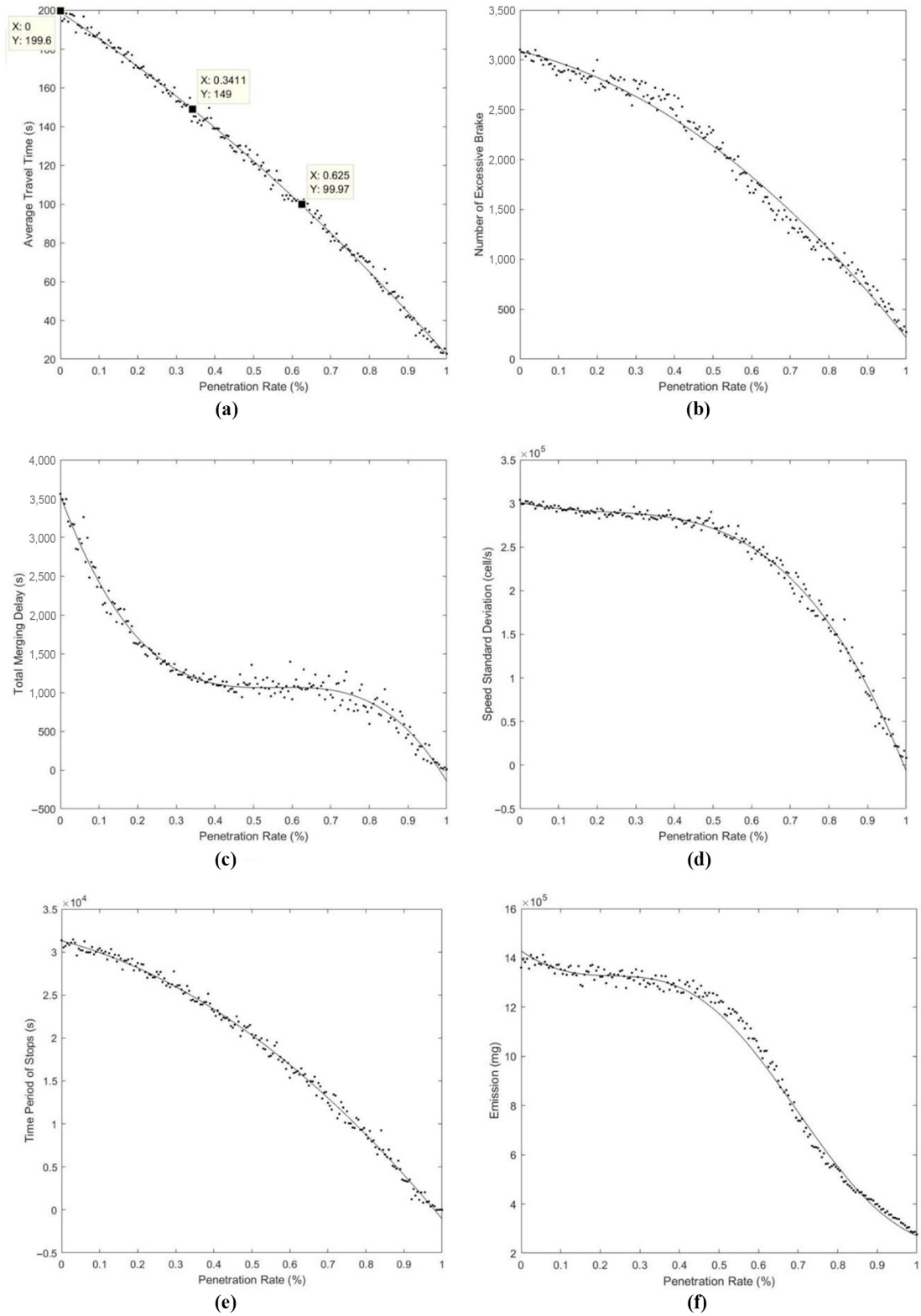

Notes: (a) Average travel time over penetration rate; (b) number of excessive brakes over penetration rate; (c) cumulative merge delay over penetration rate; (d) speed standard deviation over penetration rate; (e) time period of stops over penetration rate and (f) emission over penetration rate

Case 2: The AFV is a CAV; however, ALV is an MV.

If $G_{n,alv,t} \geq G_{security} \wedge G_{n,afv,t} \geq G_{security}$, vehicle n is able to start merging.

Otherwise, if $G_{n,alv,t} < G_{security}$:

$$V_{n,t} = V_{n,t-1} - \min(D_n, D_{comfort}, \delta_{n,t}) \tag{20}$$

and if $G_{n,afv,t} < G_{security}$:

$$V_{afv,t} = V_{afv,t-1} - \min(D_{afv}, D_{comfort}, \delta_{afv,t}) \tag{21}$$

A difference from Case 1 is that the ALVs are not indicated about this merging maneuver; thus, the deceleration of the ALV may interrupt the merging maneuver of CAV, which makes the waiting period longer.

Case 3: The AFV is an MV, and the ALV is either an MV or a CAV:

- *Scenario 1*: If $G_{n,alv,t} \geq G_{security} \wedge G_{n,afv,t} \geq G_{security} + R_c(V_{afv,t} - V_{n,t})$, vehicle n is able to start merging.
- *Scenario 2:* If $G_{n,alv,t} < G_{security}$, but the gap between ALV and AFV can accommodate the merging vehicle, namely, $G_{n,alv,t} + G_{n,afvt,t} \geq 2 \times G_{security} + R_c(V_{afv,t} - V_{n,t})$, the velocity of merging vehicle will be adjusted according to an updated front gap that is $G_{n,t} = \min(G_{n,alv,t}, G_{n,t})$. The

Figure 3 Following front gap comparison based on trajectories

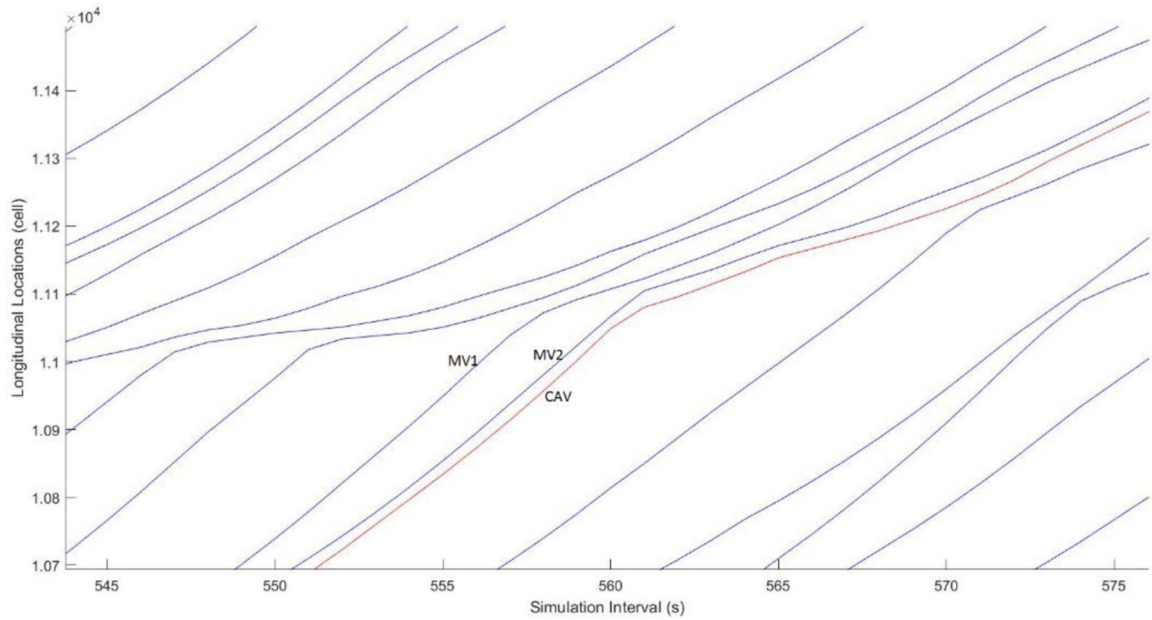

Figure 4 Following model performance analysis based on trajectories

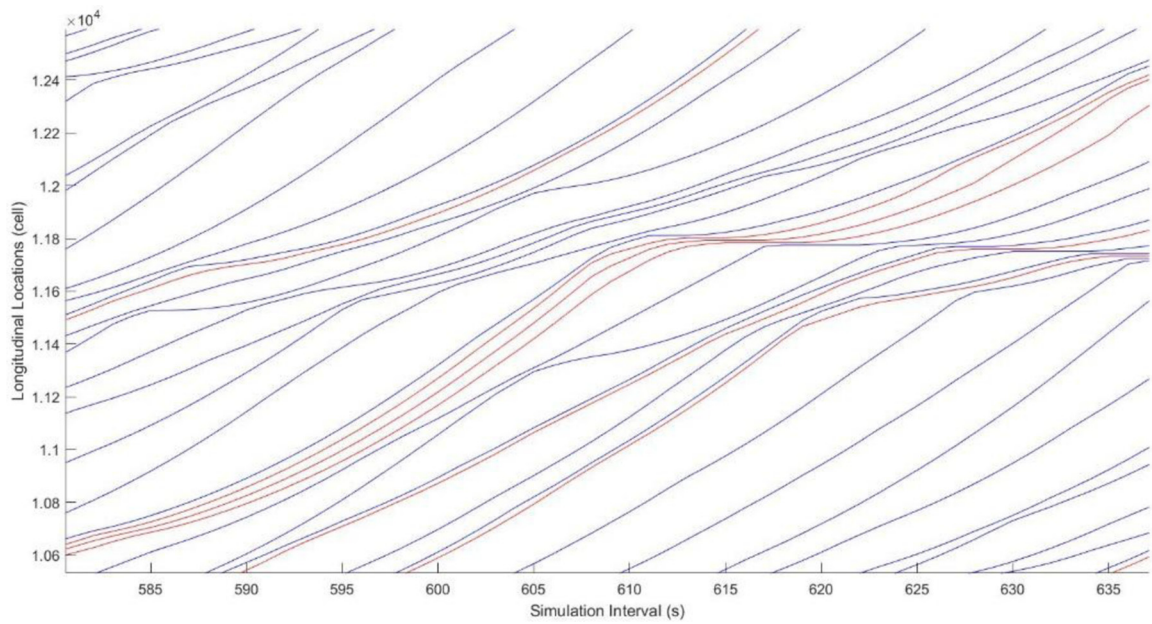

subject vehicle n will be able to merge whenever the condition mentioned in scenario is reached.

- *Scenario 3:* If $G_{n,afv,t} < G_{security}$, and the gap between ALV and AFV cannot accommodate the merging vehicle, namely, if $G_{n,alv,t} + G_{n,afvt,t} < 2 \times G_{security} + R_c(V_{afv,r} - V_{n,t})$, the subject vehicle n will have to expect to merge into a following gap, and:

$$V_{n,t} = V_{n,t-1} - \min(D_n, D_{comfort}, \delta_{n,t}) \quad (22)$$

In addition, if the AFV is followed by another CAV, this CAV will decelerate to prepare a gap for the subject vehicle n: $V_{afvf,t} = V_{afvf,t-1} - \min(D_{afvf}, D_{comfort}, \delta_{afvf,t})$. Here, $V_{afvf,t}$ denotes the velocity of the following vehicle of ALV, and D_{afvf} denotes the deceleration rate (which is illustrated in the ICA model) of the following vehicle of ALV.

To summarize, when all of these three vehicles are CAVs, a well-developed collaborative strategy can guarantee a smooth merging maneuver. While the ALV is the only MV among these three vehicles, the other two vehicles' collaborations can still perform well without the participation of the ALV. If the AFV is an MV, only a certain condition can encourage the subject CAV merge into the gap no matter ALV being CAV or not; otherwise, the collaboration will be currently terminated while

Figure 5 Priority analysis during lane-changing period

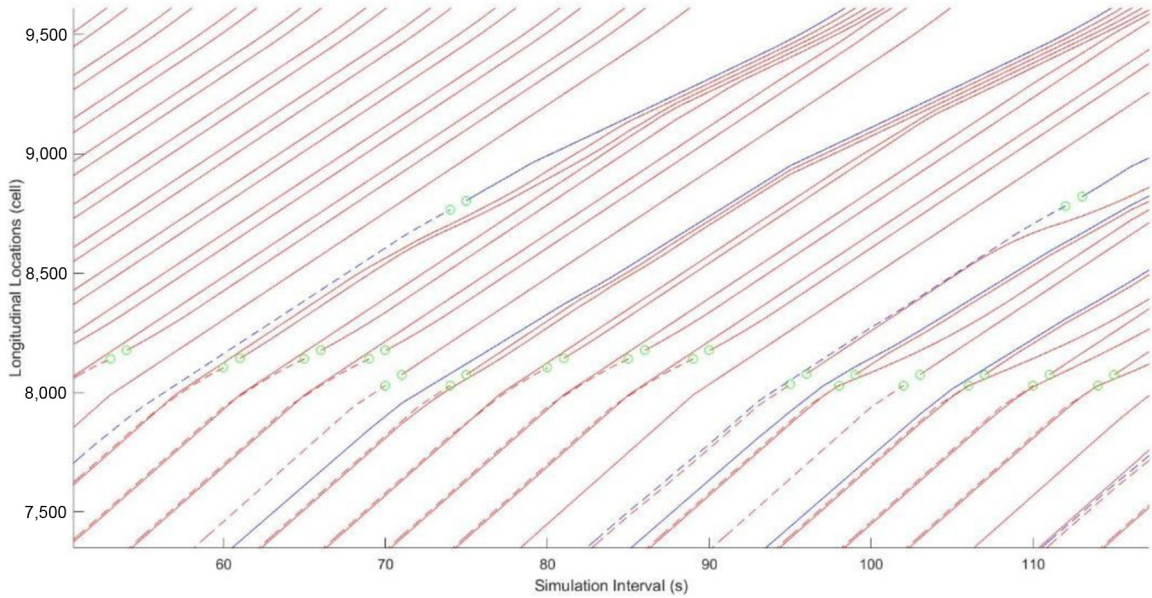

Figure 6 Cooperation between CAVs and MVs during lane-changing period

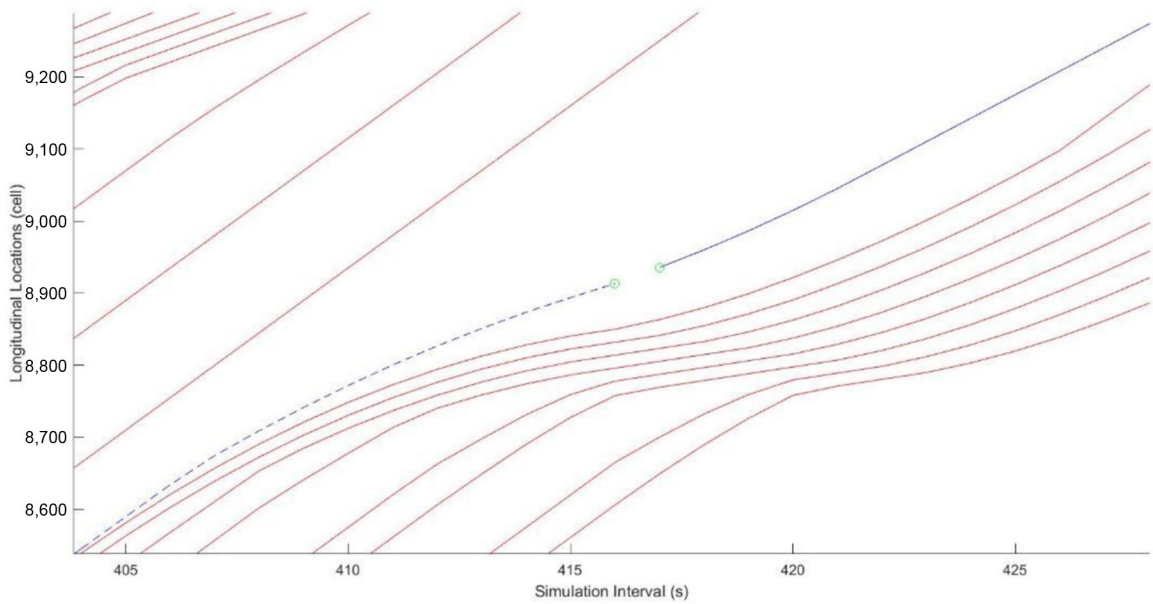

the subject CAV decelerates to look for collaborations with following vehicles.

4. Case study

4.1 Model calibration

According to traffic fundamental diagram, the speed is limited by the current density which can be transferred into current headway for individual vehicle. Greenshield's model is applied to simulate the speed limit of MVs:

$$V = V_f - \left(\frac{V_f}{K_j}\right) \times K \tag{23}$$

where V_f denotes the free flow speed which is same as the maximum speed of CAVs, K_j denotes the jam density which is assumed to be 60 vehicles per kilometer and V and K denote the actual speed and actual density, respectively. With the decrease of the headway, drivers of MVs are encouraged to drive slower than the actual speed limit to avoid rear-end crashes (Table II).

Figure 7 Trajectories without CAV's participation

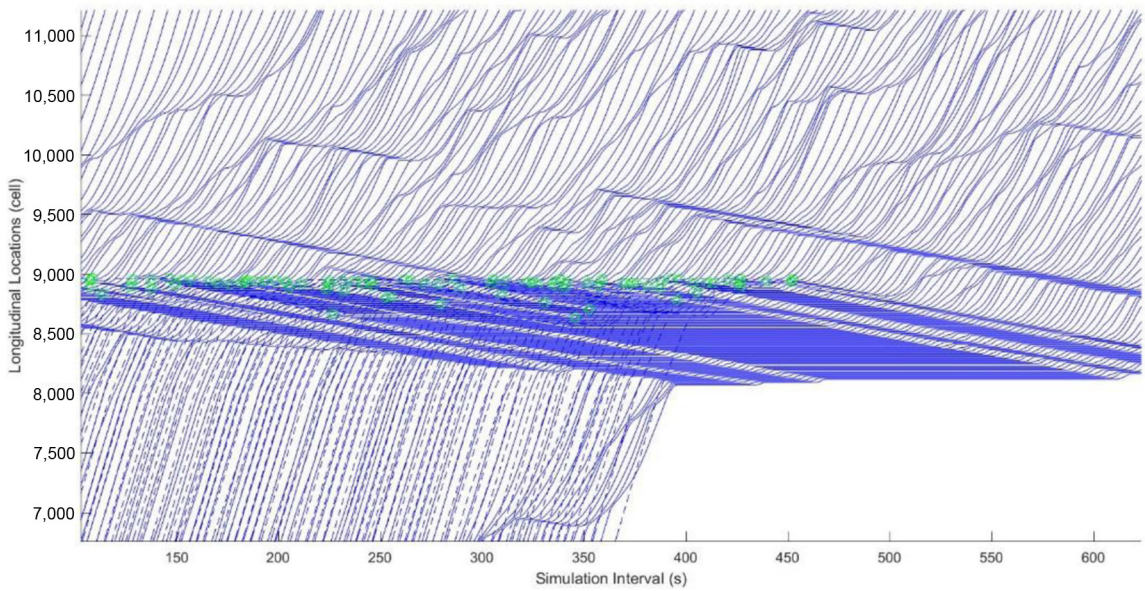

Figure 8 Trajectories with penetration rate being 100 per cent

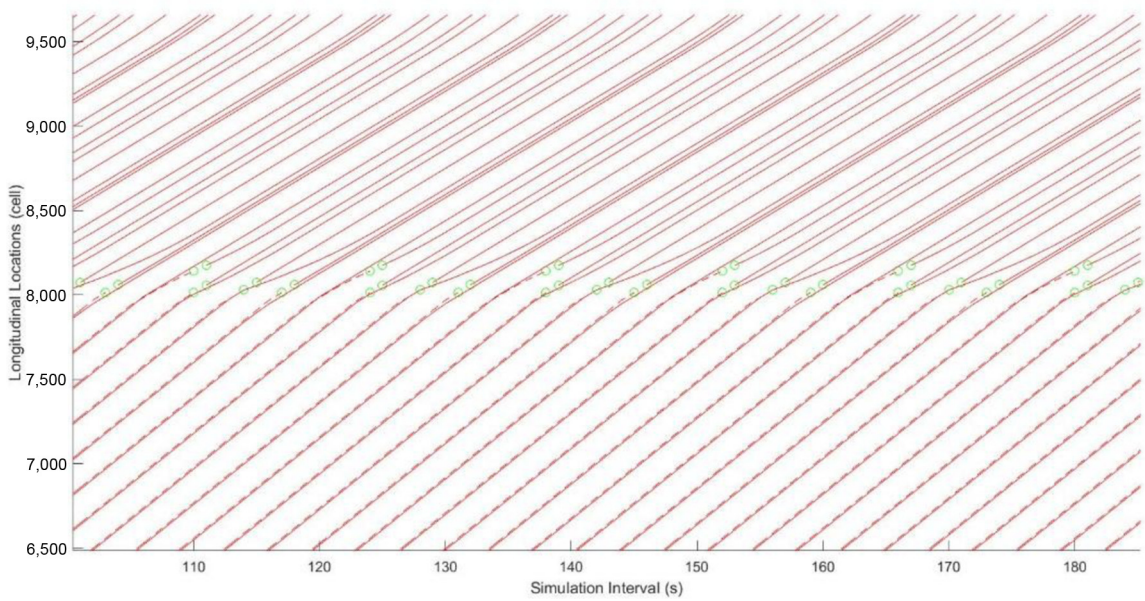

4.2 Deterministic indicators

To precisely illustrate the relationship between deterministic indicators and penetration rate, data are collected from 14 simulations while the headways are initially 3 s. The distributions of CAVs and MVs in both lanes are different among these 14 simulations to cover all scenarios of cooperation; moreover, curve fittings are done to demonstrate the relationship with equations.

These deterministic indicators are illustrated as followed:

- Travel time is an essential criterion to evaluate traffic performance according to traffic jam economic cost (Zhou *et al.*, 2017a). The average travel time is the average duration when one vehicle travels from the 8,000th cells to the 10,000th cells.
- The excessive brake represents a disturbance caused by aggressive merging maneuver downstream. We regarded comfortable deceleration rate that was suggested by American Association of State Highway and Transportation Officials (AASHTO) (2004) to be 6.8 cell/s^2 as the threshold of excessive brake; thus, the number of excessive brake is the total number of times when the deceleration rate is greater than 6.8 cell/s^2.
- Merge delay represents the time span that starts from when the merging indication is activated to whenever the merging maneuver is finished.
- Speed standard deviation is an indicator for speed variation which may cause passengers' dissatisfaction, and the speed standard deviation for vehicle n is calculated within the equation:

$$SD_n = \sqrt{\frac{\sum_{t=1}^{N}\left(V_{n,t} - \overline{V}\right)^2}{N}} \tag{24}$$

The time period of stops represents the cumulative time span when one vehicles stops (f). The quantity of emission is gained from VT-micro model that was proposed by Ahn *et al.* (2002), and has been widely used in traffic studies (Xu *et al.*, 2018; Meng *et al.*, 2010):

$$\ln(MOE_e) = \begin{cases} \sum_{i=0}^{3}\sum_{i=0}^{3}\left(L_{i,j}^{e} \times s^i \times a^j\right) & for\ a \geq 0 \\ \sum_{i=0}^{3}\sum_{i=0}^{3}\left(K_{i,j}^{e} \times s^i \times a^j\right) & for\ a < 0 \end{cases} \tag{25}$$

where $L_{i,j}^{e}$ and $K_{i,j}^{e}$ represent the coefficients in this two scenarios, whereas a and s denote acceleration and speed, respectively, as shown in Table III (Table IV).

As shown in Figure 2(a), a concave descending trend can be witnessed when penetration rate keeps increasing. The average travel time is reduced by 25 per cent when penetration rate reaches 34.1 per cent, and only half of the original travel time is needed if penetration rate reaches 62.25 per cent. In Figure 2(b), the number of excessive brake concavely decreases from 3,103 to 271 when penetration rate rises from 0 to 100 per cent. In Figure 2(c), the cumulative merge delay for all vehicles shows a non-monotonic decrease from around 3,561 s to 9 s. In Figure 2(d), the standard deviation decreases with the increase of penetration rate, and it proves that the collaboration provided by CAV can reduce the speed variation. In Figure 2(e), the time period of stops shows a concave decrease trend as penetration increases, and there will not be any vehicle stopping as a result of merging maneuver when the penetration rate reach 98.5 per cent. As shown in Figure 2(e), the y-axis denotes the total emission during the whole time span, and emission continues decreasing with the increase of percentage of CAVs involved. The trend is relatively steep when penetration rate rises from 50 to 80 per cent, which means CAVs can contribute more to reduce emission if they are the majority of vehicles. When the MV is the major part, CAVs have to give priorities to MVs frequently; thus, the collaboration that CAVs provided is relatively limited.

4.2.1 Disaggregated trajectory analysis

As shown in Figure 3, CAVs are able to tolerate much shorter headways than MVs, and the increase of density will not reduce the average speed as illustrated in Figure 2(a); in addition, trajectories of CAVs demonstrate a better performance than those of MVs when reacting the leading vehicle's deceleration,

Figure 9 Massive illustration of average travel time over penetration rate

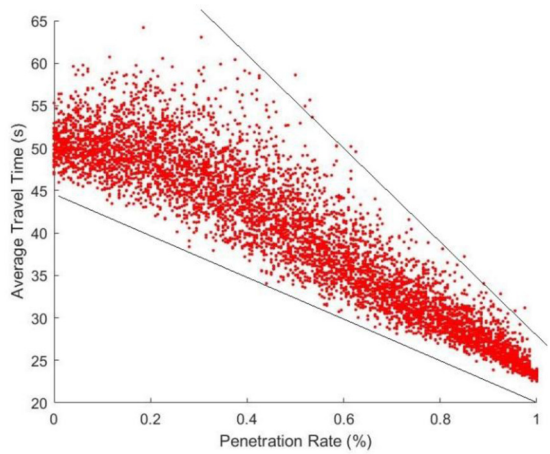

Figure 10 Massive illustration of emission over penetration rate

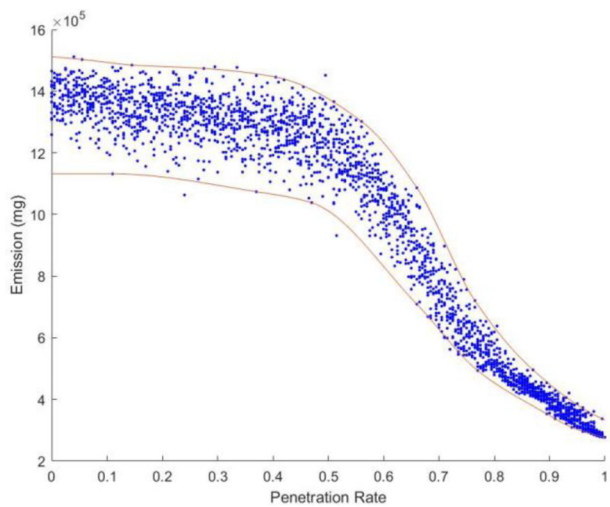

Figure 11 Velocities over locations around the work zone

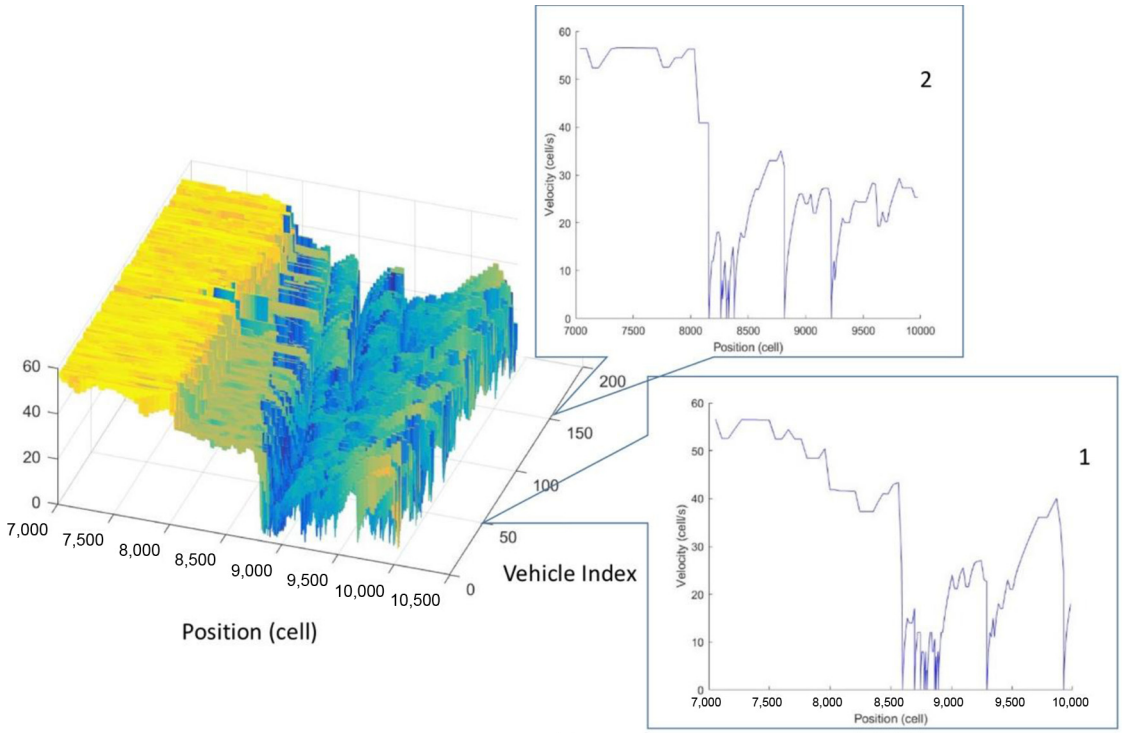

(a)

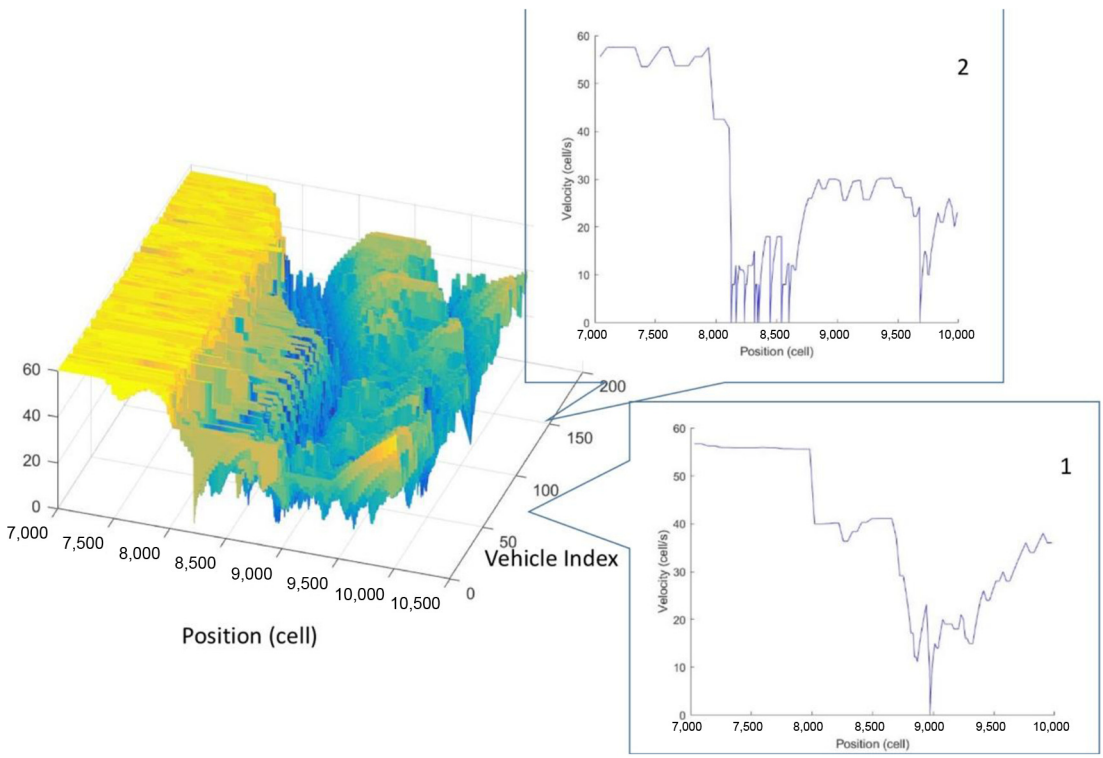

(b)

(*continued*)

Figure 11

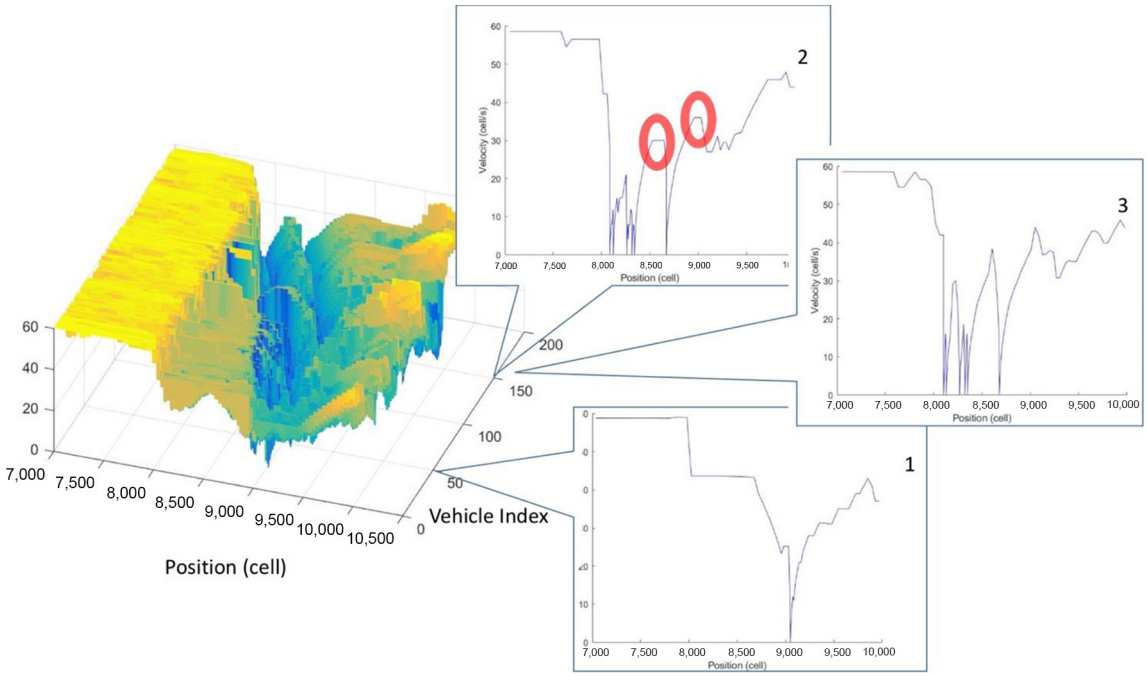

(c)

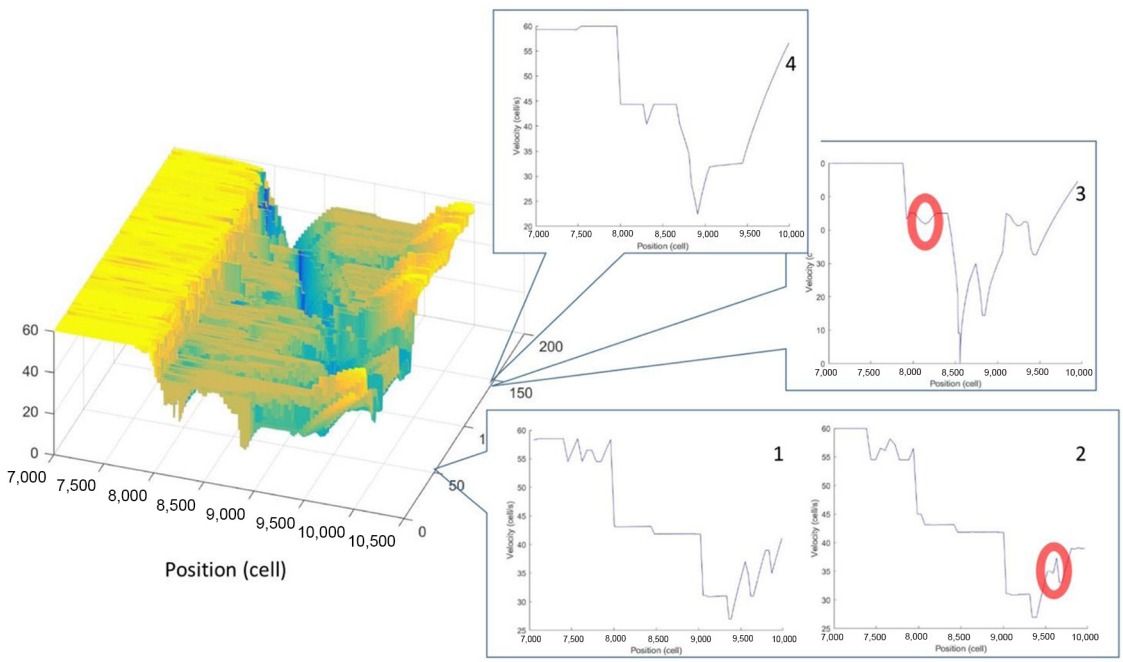

(d)

Notes: (a) Penetration rate = 0 per cent with sub-figures illustrating the velocity–location relationships of (1) the 50th vehicle which is a MV; (2) the 150th vehicle which is an MV respectively; (b) penetration rate = 30 per cent with sub-figures illustrating the velocity-location relationships of (1) the 50th vehicle which is a MV; (2) the 150th vehicle which is an MV, respectively; (c) penetration rate = 50 per cent with sub-figures illustrating the velocity–location relationships of (1) the 50th vehicle which is an MV; (2) the 150th vehicle which is a CAV; (3) the 151th vehicle which is an MV, respectively; (d) penetration rate = 80 per cent with sub-figures illustrating the velocity–location relationships of (1) the 49th vehicle which is a MV; (2) the 50th vehicle which is a CAV; (3) the 150th vehicle which is a CAV; (4) the 149th vehicle which is an MV, respectively

and there is less acceleration delay when the leading vehicle accelerates. This advantage is even clearer when CAVs are in a platoon as shown in Figure 4. While MVs suffer from the speed variations and over-braking, CAVs are able to keep a very stable trajectory, thus the speed variations due to headway variations are avoided. Consequently, not only is the average travel time reduced, but also road users' comfort is enhanced.

As shown in Figures 5 and 6, dashed lines represent the trajectories when vehicles are on Lane 1, whereas solid lines represent the trajectories when vehicles are on Lane 2, and the green circles represent the moments when vehicles on Lane 1 merge into Lane 2. In Figure 5, a CAV is able to determine whether to merge in front of or behind its adjacent vehicle according to their relative position; however, if an MV sends a lane-changing indication to the anticipated following CAV, this CAV will give priority to the MV encouraging the MV to merge, which is clearly shown in Figure 6.

Figures 7 and 8 illustrate the trajectories when penetration rate are 0 and 100 per cent, respectively. When there is no CAV participates in the simulation, the merging maneuvers bring severe disturbance to the following vhicles leading to wide moving jam; nevertheless, the cooperation among CAVs can to a large extent solve this probem, and it is shown in Figure 8.

4.3 Probabilistic indicators

Figure 9 shows the average travel time collected from more than 2,000 simulations, and the average travel time variation decreases with the penetration rate, which means that the traffic condition can be predicted in a more deterministic manner with the increase of CAVs' penetration rate. Similarly, a same trend appears on emission prediction as shown in Figure 10. The decreasing trend is similar with the one shown in Figure 8. However, the variation keeps decreasing, and it is positively related to penetration rate. It should be mentioned that both figures are depicted when initial headway is 3 s.

4.4 Traffic phase analysis

Figure 11 demonstrates the velocities at different longitudinal positions around the work zone under CAVs' penetration rates of (a) 0, (b) 30, (c) 50 and (d) 80 per cent, respectively. Their sub-figures illustrate the velocities of the 50th vehicle and the 150th vehicle representing the downstream vehicles and upstream vehicles, respectively. The velocities of their surrounding CAVs are also demonstrated for comparison purpose when penetration rate is 50 and 80 per cent. The dashed lines that are perpendicular to the x-axis represent the start position of advance warning zone and the end position of termination area, respectively. As shown in Figure 11(a), a severe traffic jam appears within the work zone area, and most of vehicles still travel with low speeds even though they have passed the work zone by 500 cells. As can be seen from two sub-figures, the upstream vehicles (represented by sub-figure 2) suffer a more severe disturbance than downstream vehicles (represented by sub-figure 1) because disturbances propagate along the platoon. In Figure 11(b), vehicles are able to accelerate to relatively high speed after suffering a severe disturbance even though vehicles are still within the work zone area with the help of a few (taking around 30 per cent of total number of vehicles) CAVs' collaborations; however, the speeds are still lower than normal speed limit after passing the work zone, but this problem can be alleviated when there are more CAVs in the platoon, as shown in Figure 11(c). With the collaboration provided by CAVs, MVs suffer less disturbances, as shown in sub-figure 1. Sub-figures 2 and 3 illustrate the velocities of two successive vehicles that consist of a leading CAV and a following MV, and the main differences are circled in the figure. CAV has higher peak speed than MV at same condition because CAVs can handle shorter front gap after precise calculations. In that case, vehicles can narrow the front gaps effectively. When penetration rate reaches a relatively high level, most of disturbances are able to be avoided at high level (80 per cent) of penetration rate. In Figure 11(d), sub-figures 1 and 2 and sub-figures 3 and 4 illustrate two pairs of successive vehicles both consisting of a leading MV and a following CAV. The circled areas in sub-figures 3 and 4 illustrate the advantage that CAVs can decelerate with a relatively small deceleration rate to avoid passengers' dissatisfaction while avoiding the rear-end crash at the same time. Hence, disturbances cumulated along the platoon can be effectively avoided; moreover, most of vehicles can accelerate to its original speed after leaving the work zone.

5. Conclusion

Work zones bring negative impact on freeway traffic, and a number of problems emerge, such as long travel time, high speed variation, driver's dissatisfaction and traffic congestion. In this research, for the first time, we develop a CCAM introducing a collaborative component of CAVs to simulate a highway work zone system. Results are collected from different penetration rates for comparison purposes, and positive effects are demonstrated. The average travel time decreases by 25 and 50 per cent when penetration rate reaches 34.1 and 62.25 per cent, respectively. The variability of these indicators also has significant decrease as the penetration rate of CAVs goes up. We also extract some of the trajectories to analyze the reason for these improvements, and it clearly reveals how CAVs harmonize traffic flow dynamics.

References

Adeli, H. and Jiang, X. (2003), "Neuro-fuzzy logic model for freeway work zone capacity estimation", *Journal of Transportation Engineering*, Vol. 129 No. 5, pp. 484-493.

Ahn, K., Rakha, H., Trani, A. and Van Aerde, M. (2002), "Estimating vehicle fuel consumption and emissions based on instantaneous speed and acceleration levels", *Journal of Transportation Engineering*, Vol. 128 No. 2, pp. 182-190.

American Association of State Highway and Transportation Officials (AASHTO) (2004), *A Policy on Geometric Design of Highways and Street*, 5th Ed., Washington, DC.

Garber, N. and Zhao, M. (2002), "Distribution and characteristics of crashes at different work zone locations in Virginia", *Transportation Research Record: Journal of the Transportation Research Board*, Vol. 1794, pp. 19-25.

Hidas, P. (2002), "Modelling lane changing and merging in microscopic traffic simulation", *Transportation Research Part C: Emerging Technologies*, Vol. 10 Nos 5/6, pp. 351-371.

Jiang, X. and Adeli, H. (2004a), "Clustering-neural network models for freeway work zone capacity estimation",

International Journal of Neural Systems, Vol. 14 No. 3, pp. 147-163.

Jiang, X. and Adeli, H. (2004b), "Object-Oriented model for freeway work zone capacity and queue delay estimation", *Computer-Aided Civil and Infrastructure Engineering*, Vol. 19 No. 2, p. 144-156.

Khattak, A.J., Khattak, A.J. and Council, F.M. (2002), "Effects of work zone presence on injury and non-injury crashes", *Accident; Analysis and Prevention*, Vol. 34 No. 1, pp. 19-29.

Laval, J.A. and Daganzo, C.F. (2006), "Lane-changing in traffic streams", *Transportation Research Part B: Methodological*, Vol. 40 No. 3, pp. 251-264.

Macadam, C.C. (2003), "Understanding and modeling the human driver", *Vehicle System Dynamics*, Vol. 40 Nos 1/3, pp. 101-134.

Meng, Q. and Weng, J. (2010), "Cellular automata model for work zone traffic", *Transportation Research Record: Journal of the Transportation Research Board*, Vol. 2188 No. 1, pp. 131-139.

Meng, Q. and Weng, J. (2011), "A genetic algorithm approach to assessing work zone casualty risk", *Safety Science*, Vol. 49 Nos 8/9, pp. 1283-1288.

Meng, Q. and Weng, J. (2011), "An improved cellular automata model for heterogeneous work zone traffic", *Transportation Research Part C: Emerging Technologies*, Vol. 19 No. 6, pp. 1263-1275.

Meng, Q., Weng, J. and Qu, X. (2010), "A probabilistic quantitative risk assessment model for long term work zone crashes", *Accident Analysis and Prevention*, Vol. 42 No. 6, pp. 1866-1877.

Nagel, K. and Schreckenberg, M. (1992), "A cellular automaton model for freeway traffic", *Journal de Physique I*, Vol. 2 No. 12, pp. 2221-2229.

Qu, X., Wang, S. and Zhang, J. (2015), "On the fundamental diagram for freeway traffic: a novel calibration approach for single-regime models", *Transportation Research Part B*, Vol. 73, pp. 91-102.

Qu, X., Zhang, J. and Wang, S. (2017), "On the stochastic fundamental diagram for freeway traffic: model development, analytical properties, validation, and extensive applications", *Transportation Research Part B*, Vol. 104, pp. 256-271.

Rouphail, N.M., Yang, Z.S. and Fazio, J. (1988), *Comparative Study of Short-and Long-Term Urban Freeway Work Zones*, Vol. 1163.

Wang, J., Hughes, W., Council, F. and Paniati, J. (1996), "Investigation of highway work zone crashes: what we know and what we don't know", *Transportation Research Record: Journal of the Transportation Research Board*, Vol. 1529, pp. 54-62.

Weng, J. and Meng, Q. (2014), "Rear-end crash potential estimation in the work zone merging areas", *Journal of Advanced Transportation*, Vol. 48 No. 3, pp. 238-249.

Weng, J. and Yan, X. (2016), "Probability distribution-based model for work zone capacity prediction", *Journal of Advanced Transportation*, Vol. 50 No. 2, pp. 165-179.

Xu, Z., Wei, T., Easa, S., Zhao, X. and Qu, X. (2018), "Modeling relationship between truck fuel consumption and driving behavior using data from internet of vehicles", *Computer-Aided Civil and Infrastructure Engineering*, Vol. 33 No. 3, pp. 209-219.

Zhou, M., Qu, X. and Jin, S. (2017a), "On the impact of cooperative autonomous vehicles in improving freeway merging: a modified intelligent driver model based approach", *IEEE Transactions on Intelligent Transportation Systems*, Vol. 18 No. 6, pp. 1422-1428.

Zhou, M., Qu, X. and Li, X. (2017b), "A recurrent neural network based microscopic car following model to predict traffic oscillation", *Transportation Research Part C*, Vol. 84, pp. 245-264.

Further reading

Jiang, X. and Adeli, H. (2003), "Freeway work zone traffic delay and cost optimization model", *Journal of Transportation Engineering*, Vol. 129 No. 3, pp. 230-241.

Karim, A. and Adeli, H. (2003), "Radial basis function neural network for work zone capacity and queue estimation", *Journal of Transportation Engineering*, Vol. 129 No. 5, pp. 494-503.

Corresponding author

Xiaobo Qu can be contacted at: drxiaoboqu@gmail.com